Complete catalog of ground-state diagrams for the general three-state lattice-gas model with nearest-neighbor interactions on a square lattice

SCHOLARONE™
Manuscripts

Complete catalog of ground-state diagrams for the general three-state lattice-gas model with nearest-neighbor interactions on a square lattice

Daniel Silva[1] and Per Arne Rikvold[1,2]

[1] *Department of Physics, Florida State University, Tallahassee, FL 32306-4350,USA*

[2] *PoreLab, NJORD Centre, Department of Physics,*
University of Oslo, P.O. Box 1048 Blindern, 0316 Oslo, Norway

Abstract

The ground states of the general three-state lattice-gas (equivalently, $S = 1$ Ising) model with nearest-neighbor interactions on a square lattice are explored in the full, five-dimensional parameter space of three interaction constants and two generalized chemical potentials or fields. The complete catalog of fifteen topologically different ground-state diagrams (zero-temperature phase diagrams), which show the regions of stability of the different ground states in the full parameter space of the model, is obtained and discussed in both lattice-gas and Ising-spin language. The results extend those of a recent study in a reduced parameter space [V. F. Fefelov, *et al.*, *Phys. Chem. Chem. Phys.*, 2018, **20**, 10359–10368], which identified six topologically different ground-state diagrams.

I. INTRODUCTION

Many physical, chemical, or social systems can be described as a lattice or a more general network, whose sites carry a discrete variable with a finite number of possible states. The simplest example is the $S = 1/2$ Ising model [1–3], in which each site can take one of two values. Common interpretations in physics and chemistry include opposite directions of a magnetic or electric dipole moment or "spin" ($\sigma \in \{-1, +1\}$), or the absence or presence of an atom or a molecule ($c \in \{0, 1\}$). In the social sciences, the states might, e.g., represent opinions, population groups, or languages [4].

In the present paper we consider the more complex case of three possible states, known as the $S = 1$ Ising model ($\sigma \in \{-1, 0, +1\}$) or, equivalently, the three-state lattice-gas (LG) model with states A, B, and vacancy (0). The spin representation has been used to describe magnetic or dielectric systems with local triplet states [5] or the λ transition in He^3-He^4 mixtures [6]. In its LG form, the model has been used extensively to study two-component adsorption at solid-gas [7] and solid-liquid [8–10] interfaces, as well as spatially complex mixtures of protons, neutrons, and voids ("nuclear pasta") thought to exist in the inner crust of neutron stars [11].

Models using such discrete-state representations are typically defined by an effective Hamiltonian including "interaction constants" representing the tendency of state variables on neighboring sites to take equal or different values, and external "chemical potentials" or "fields" that determine the individual energies of the state variables. While the two-state model with nearest-neighbor interactions contains one interaction constant and one field, the general three-state model contains three interaction constants and two fields. The tendency to seek an ordered minimum-energy configuration, or *ground state*, is counterbalanced by a "temperature" parameter encouraging disorder. Due to this competition between order and disorder, complex phenomena, including continuous or discontinuous phase transitions, occur at nonzero temperatures. However, aspects of the ground-state configurations are typically observable (at least as local fluctuations), even at quite high temperatures. A study of the *ground-state diagrams* (zero-temperature phase diagrams), formed by the lines or planes in a parameter space of interaction constants and fields that separate the regions of stability of the different ground states, is therefore a natural starting point for detailed studies of equilibrium or nonequilibrium phenomena at nonzero temperatures. The ground-

state diagram can be likened to the foundation, on which the "building" representing the full, finite-temperature phase diagram is supported.

For the two-dimensional triangular lattice, complete analysis of the topologically different ground-state diagrams produced by different parameter values in the three-state LG model with nearest-neighbor interactions and the equivalent $S = 1$ Ising model were presented in Refs. [8] and [12], respectively. For the simpler, two-dimensional square lattice, ground-state diagrams for a related LG model with nearest- and next-nearest neighbor repulsive interactions were obtained by Huckaby and Kowalski [13]. Complex ground-state diagrams for a mixed $S = 1$ and $S = 2$ (five-state) model on a square lattice were obtained for several reduced parameter sets by De La Espriella *et al.* [14]. Very recently, Fefelov *et al.* presented the six possible phase diagrams for the three-state LG model in the special case of vanishing interactions between particles of opposite kinds, representing an additive gas mixture [7]. However, to the best of our knowledge, no full enumeration of topologically different ground-state diagrams for the square lattice in the general case of three non-vanishing interaction constants has previously been presented. The purpose of the present paper is to provide such a complete description in both LG and Ising-spin language for this important lattice, whose physical realizations include the (100) planes of the three-dimensional body-centered and face-centered cubic crystal lattices.

The rest of this paper is organized as follows. The model Hamiltonian is presented in Sec. II, with the spin formulation in Subsec. II A and the LG formulation in Subsec. II B, where the relations between the model parameters in the two representations are also given. Section III consists of three subsections. The six possible ground states are reviewed in Subsec. III A, and phase diagrams in six different asymptotic strong-field limits are described in Subsec. III B. Our main results, the complete enumeration and description of the fifteen topologically different ground-state diagrams, including the intermediate and weak field limits where the asymptotic regions meet, are given in Subsec. III C. A short summary and our conclusions are given in Sec. IV.

II. MODEL

A. Ising-spin formulation

The most general form for the $S = 1$ Ising Hamiltonian with nearest-neighbor pairwise interactions takes the form,

$$\mathcal{H}_{S=1} = -J \sum_{\langle i,j \rangle} p_i p_j - K \sum_{\langle i,j \rangle} q_i q_j - L \sum_{\langle i,j \rangle} (q_i p_j + p_i q_j)$$
$$+ D \sum_i q_i - H \sum_i p_i \, . \tag{1}$$

Here, $\sum_{\langle i,j \rangle}$ denotes summation over all nearest-neighbor pairs, where $p_i \in \{-1, 0, 1\}$ and $q_i = p_i^2$. The parameters J and H are analogous to the single interaction constant and the external field in the $S = 1/2$ Ising model, respectively. [See Eq. (2) below.] The interaction constant $J > 0$ and $J < 0$ correspond to the uniform ferromagnetic (FM) case and the checkerboard antiferromagnetic (AFM) case, respectively, and the field H distinguishes between positive and negative p_i. The "crystal field" D distinguishes between zero and nonzero p_i, with $D < 0$ denoting preference for $q_i = 1$. $K < 0$ denotes preference for bonds with at least one zero spin, while $K > 0$ denotes a preference for nearest neighbors being nonzero, irrespective of sign. $L > 0$ corresponds to a preference for ferromagnetic ordering with $p_i = +1$. This most general $S = 1$ Ising model is invariant under the transformation $L \to -L, H \to -H, p_i \to -p_i$. Its ground states and ground-state diagrams were studied on a triangular lattice in Refs. [8] and [12].

Setting $L = 0$, one gets the Blume-Emery-Griffiths (BEG) model [6], while setting $K = L = 0$ leads to the Blume-Capel (BC) model [5]. Additionally setting $D = 0$ and limiting the spins to up or down, $\sigma_i \in \{-1, +1\}$, one obtains the $S = 1/2$ Ising model, known as the "hobby horse" of magnetic systems [3],

$$\mathcal{H}_{\text{Ising}} = -J \sum_{\langle i,j \rangle} \sigma_i \sigma_j - H \sum_i \sigma_i \, . \tag{2}$$

B. Lattice-gas formulation

The $S = 1$ Ising model can be mapped to a three-state (A, B, and vacancy 0) LG model. It can represent two gases with molecules of types A and B or two solutes and a solvent.

Interactions between molecules of types A and B are denoted ϕ_{AB}, while interactions between molecules of same type are denoted ϕ_{AA} and ϕ_{BB}. The Ising Hamiltonian can be transformed to a lattice-gas Hamiltonian by introducing the local concentration variables,

$$c_i^A = \frac{1}{2}(q_i + p_i) \tag{3}$$

and

$$c_i^B = \frac{1}{2}(q_i - p_i) , \tag{4}$$

and defining the interaction energies ϕ_{AA}, ϕ_{BB}, and ϕ_{AB} and the chemical potentials μ_A and μ_B , as [12]

$$\phi_{AA} = J + K + 2L$$
$$\phi_{BB} = J + K - 2L$$
$$\phi_{AB} = K - J \tag{5}$$
$$\mu_A = H - D$$
$$\mu_B = -H - D .$$

From these definitions we get the grand-canonical LG Hamiltonian,

$$\mathcal{H}_{\text{LG}} = -\phi_{AA} \sum_{\langle i,j \rangle} c_i^A c_j^A - \phi_{BB} \sum_{\langle i,j \rangle} c_i^B c_j^B - \phi_{AB} \sum_{\langle i,j \rangle} (c_i^A c_j^B + c_i^B c_j^A)$$
$$-\mu_A \sum_i c_i^A - \mu_B \sum_i c_i^B . \tag{6}$$

The special case of $\phi_{AB} = 0$, or equivalently $K = J$, was recently studied in Ref. [7].

The mapping defined by Eqs. (3) − (5) is trivially inverted to yield

$$p_i = c_i^A - c_i^B$$
$$q_i = c_i^A + c_i^B \tag{7}$$

and

$$J = \frac{1}{4}(\phi_{AA} - 2\phi_{AB} + \phi_{BB})$$
$$K = \frac{1}{4}(\phi_{AA} + 2\phi_{AB} + \phi_{BB})$$
$$L = \frac{1}{4}(\phi_{AA} - \phi_{BB}) \tag{8}$$
$$D = -\frac{1}{2}(\mu_A + \mu_B)$$
$$H = \frac{1}{2}(\mu_A - \mu_B) .$$

III. GROUND-STATE CALCULATION

A. Ground states

The density conjugate to the chemical potential μ_X is the coverage $\theta_X = N^{-1} \sum_i c_i^X$, where N is the total number of lattice sites. From Eq. (7) we note that $p_i = +1$ means $c_i^A = 1$ and $c_i^B = 0$, and opposite for $p_i = -1$. The macroscopic densities conjugate to the fields H and $-D$ are the magnetization $P = N^{-1} \sum_i p_i$ and the quadrupole moment $Q = N^{-1} \sum_i q_i$, respectively. Specific phases are identified by their corresponding values of P and Q by $(X \times Y)_P^Q$. Here, X and Y denote the periodicities in the two lattice directions, a notation common in surface science. The energy per lattice site of a particular phase is found by evaluating the Hamiltonian for the corresponding configuration,

$$E_{(X \times Y)_P^Q} = \frac{\mathcal{H}_{(X \times Y)_P^Q}}{N} . \tag{9}$$

The ground state is the one with the minimum energy. It is a function of the parameters $J, K, L, D,$ and H (or $\phi_{AA}, \phi_{BB}, \phi_{AB}, \mu_A,$ and μ_B),

$$E_{\text{gs}}(J, K, L, D, H) = \min\{E_{(X \times Y)_P^Q}\} . \tag{10}$$

Candidate ordered phases are chosen among those that can be reached from the uniform (a.k.a. disordered) (1×1) phases by continuous phase transitions, as determined by group-theoretical arguments [15, 16]. In the absence of interactions beyond nearest neighbors, the only ordered phases possible have the $(\sqrt{2} \times \sqrt{2})$ symmetry [16], which divides the lattice into two interpenetrating sublattices. In spin language, these checkerboard phases are commonly called *antiferromagnetic* (AFM). For different values of the five parameters, six different phases can be formed. These are shown in Fig. 1. There are three uniform phases, $(1 \times 1)_1^1$ (all A), $(1 \times 1)_{-1}^1$ (all B), and the empty lattice $(1 \times 1)_0^0$ (all 0), and three ordered checkerboard (AFM) phases, $(\sqrt{2} \times \sqrt{2})_0^1$ (A and B), $(\sqrt{2} \times \sqrt{2})_{1/2}^{1/2}$ (A and 0), and $(\sqrt{2} \times \sqrt{2})_{-1/2}^{1/2}$ (B and 0). These ground states, along with their corresponding values of Q, P, θ_A, θ_B and their energies per lattice site, are shown in Table I, using both Ising and LG notation.
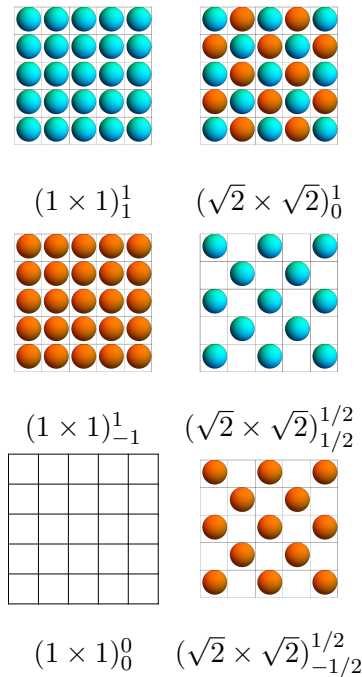
6

FIG. 1: Configurations corresponding to the six possible ground states for the model defined in Eqs. (1) and (6). The uniform phases, shown in the left column, are $(1 \times 1)_1^1$ (all A), $(1 \times 1)_{-1}^1$ (all B), and $(1 \times 1)_0^0$ (empty lattice). The ordered phases, shown in the right column, are $(\sqrt{2} \times \sqrt{2})_0^1$ (A and B), $(\sqrt{2} \times \sqrt{2})_{1/2}^{1/2}$ (A and 0), and $(\sqrt{2} \times \sqrt{2})_{-1/2}^{1/2}$ (B and 0).

B. Asymptotic results

The phase boundaries in the five-dimensional parameter space are found by pair-wise equating the energy per site of different possible ground states. The ground state is uniform in three asymptotic strong-field limits. As $H \to +\infty$ at constant D, the ground state is $(1 \times 1)_1^1$, while for $H \to -\infty$ at constant D, it is $(1 \times 1)_{-1}^1$. Similarly, for $D \to +\infty$ at constant H, empty sites become energetically favorable, and the ground state is $(1 \times 1)_0^0$.

In three other asymptotic directions, the Hamiltonian reduces to the $S = 1/2$ Ising model, Eq. (2), but with effective parameters, $\hat{J}$ and $\hat{H}$, which are functions of the five parameters of the full Hamiltonian, Eqs. (1) and (6),

$$\hat{\mathcal{H}}_{\mathcal{I}} = -\hat{J} \sum_{\langle i,j \rangle} \sigma_i \sigma_j - \hat{H} \sum_i \sigma_i \ . \tag{11}$$

As $D \to -\infty$, $p_i = q_i = 0$ becomes energetically unfavorable, and the Hamiltonian

TABLE I: The six possible ground states and their properties, in both Ising and LG language.

State	Config.	Q	P	θ_A	θ_B	Energy per site
$(1 \times 1)^1_1$	AA	1	1	1	0	$-2J - 2K - 4L + D - H$
	AA					$= -2\phi_{AA} - \mu_A$
$(1 \times 1)^1_{-1}$	BB	1	-1	0	1	$-2J - 2K + 4L + D + H$
	BB					$= -2\phi_{BB} - \mu_B$
$(1 \times 1)^0_0$	00	0	0	0	0	0
	00					
$(\sqrt{2} \times \sqrt{2})^1_0$	AB	1	0	1/2	1/2	$2J - 2K + D$
	BA					$= -2\phi_{AB} - \dfrac{1}{2}(\mu_A + \mu_B)$
$(\sqrt{2} \times \sqrt{2})^{1/2}_{1/2}$	A0	1/2	1/2	1/2	0	$\dfrac{1}{2}(D - H) = -\dfrac{1}{2}\mu_A$
	0A					
$(\sqrt{2} \times \sqrt{2})^{1/2}_{-1/2}$	B0	1/2	$-1/2$	0	1/2	$\dfrac{1}{2}(D + H) = -\dfrac{1}{2}\mu_B$
	0B					

reduces to Eq. (11) with

$$\sigma_i = p_i = \pm 1$$
$$\hat{J} = J \qquad (12)$$
$$\hat{H} = H + 4L \ .$$

This is just the $S = 1/2$ Ising model with the original interaction constant J and the field shifted by $-4L$. It is FM or AFM, depending on whether J is positive or negative, respectively.

As $H \to +\infty$ and $D \to +\infty$ ($\mu_B \to -\infty$ at constant μ_A), it is energetically unfavorable to have $p_i = -1$ (i.e., B molecules are desorbed). Thus $p_i = q_i \in \{1, 0\}$, and the model reduces to the two-state LG model for single-component adsorption of A. The corresponding

effective $S = 1/2$ Ising model has

$$\sigma_i = 2q_i - 1 = 2p_i - 1$$

$$\hat{J} = \frac{1}{4}(J + K + 2L) = \frac{1}{4}\phi_{AA} \tag{13}$$

$$\hat{H} = \frac{1}{2}(H - D) + (J + K + 2L) = \frac{1}{2}(\mu_A + 2\phi_{AA}) \ .$$

If $\phi_{AA} < 0$, the ordered ground state, $(\sqrt{2} \times \sqrt{2})_{1/2}^{1/2}$ (A and 0) will occur between the two uniform ground states that are stable in the asymptotic limit of $\mu_B \to -\infty$.

Analogously, as $H \to -\infty$ and $D \to +\infty$ ($\mu_A \to -\infty$ at constant μ_B), then $p_i = -q_i \in \{-1, 0\}$. Molecules of type A become energetically unfavorable and are desorbed. The model reduces to the two-state LG model for single-component adsorption of B. The corresponding effective $S = 1/2$ Ising model has

$$\sigma_i = 2q_i - 1 = -2p_i - 1$$

$$\hat{J} = \frac{1}{4}(J + K - 2L) = \frac{1}{4}\phi_{BB} \tag{14}$$

$$\hat{H} = \frac{1}{2}(-H - D) + (J + K - 2L) = \frac{1}{2}(\mu_B + 2\phi_{BB}) \ .$$

If $\phi_{BB} < 0$, the ordered ground state, $(\sqrt{2} \times \sqrt{2})_{-1/2}^{1/2}$ (B and 0) will occur between the two uniform ground states that are stable in the asymptotic limit of $\mu_A \to -\infty$.

We now have the information necessary to construct the complete set of topologically different ground-state diagrams that determine the stability regions of the individual ground states in the full parameter space of the model.

C.   Topologically different ground-state diagrams

Starting from one of the three uniform ground states, and proceeding toward one of the other two, one can determine which, if any, of the ordered states first becomes lower in energy than the uniform states. The values of the fields H and D that mark the transitions between different ground states depend on the values of the interaction parameters J, K, and L. Different values of these parameters therefore lead to topologically different ground-state diagrams in the $\{H, D\}$ plane.

9

TABLE II: Main regions in the $\{k, \ell\}$ plane.

Region	Ising condition	Lattice-gas condition
I	$-1 - k < 2\ell < 1 + k$	$\phi_{AA} > 0, \phi_{BB} > 0$
II	$2\ell > -1 - k$ and $2\ell > 1 + k$	$\phi_{AA} > 0, \phi_{BB} < 0$
III	$2\ell < -1 - k$ and $2\ell < 1 + k$	$\phi_{AA} < 0, \phi_{BB} > 0$
IV	$1 + k < 2\ell < -1 - k$	$\phi_{AA} < 0, \phi_{BB} < 0$

In the rest of this paper we will for convenience sometimes use the normalized interactions and fields: $j = J/|J|$, $k = K/|J|$, $\ell = L/|J|$, $h = H/|J|$, and $d = D/|J|$. We now proceed to show that, in terms of h and d, there are fifteen topologically different ground-state diagrams.

Our first classification is in terms of the ground states for the FM ($j = +1$) and AFM ($j = -1$) cases in the $d \to -\infty$ limit. In the FM case, there is a direct transition between the uniform $(1 \times 1)_1^1$ and $(1 \times 1)_{-1}^1$ ground states at $h = -4\ell$, while in the AFM case these uniform phases are separated by a region of the checkerboard $(\sqrt{2} \times \sqrt{2})_0^1$ (A and B) phase in the range $-4\ell + 4j < h < -4\ell - 4j$.

In both the FM and AFM cases, the $\{k, \ell\}$ plane is divided into four main regions, denoted I-IV. The inequalities that define these four regions are shown in Table II in both Ising and LG language. After this division of the $\{k, \ell\}$ plane into four main regions, the remaining subdivisions are made according to the different topologies the ground-state diagrams can have in the $\{h, d\}$ plane. In Fig. 2(a) we show the five regions in the $\{k, \ell\}$ plane that correspond to topologically distinct ground-state diagrams in the FM case. Likewise, in Fig. 3(a) we show the ten regions in the $\{k, \ell\}$ plane that correspond to topologically distinct ground-state diagrams in the AFM case. In both cases, the lines that separate different regions correspond to degenerate ground-state diagrams, intermediate between the adjoining topologies. In these figures, the k axis corresponds to the BEG model, and the origin to the BC model.
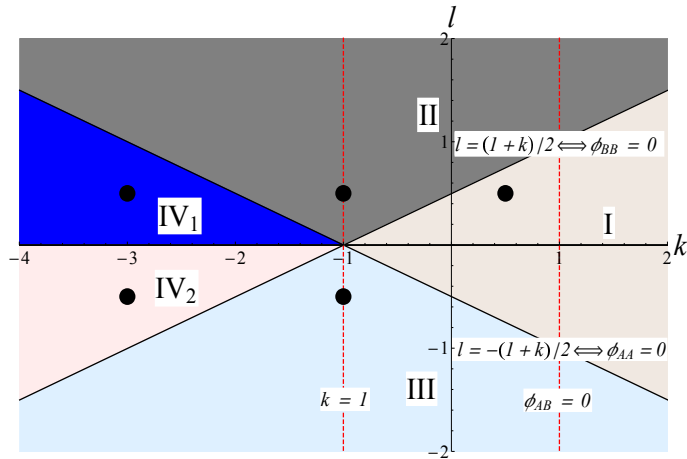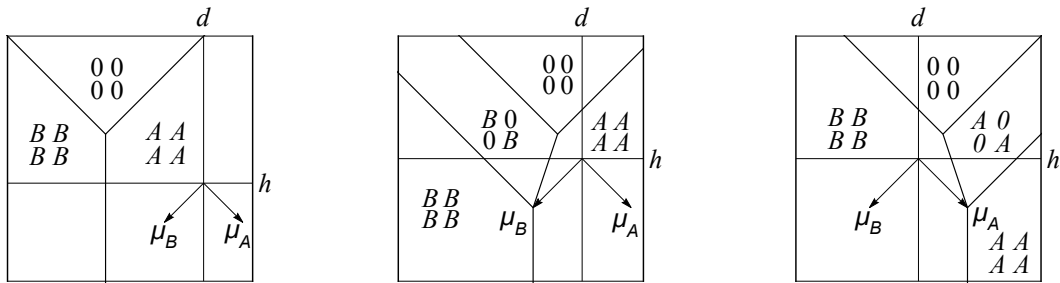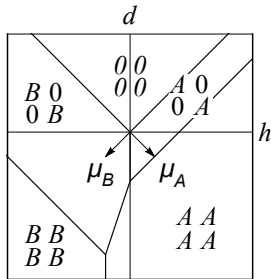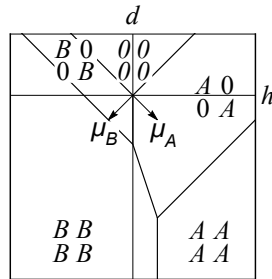
(a) The regions in the $\{k, \ell\}$ plane in the FM case.

(b) I. $\{k, \ell\} = \{0.5, 0.5\}$.   (c) II. $\{k, \ell\} = \{-1.0, 0.5\}$.   (d) III. $\{k, \ell\} = \{-1.0, -0.5\}$.

(e) IV$_1$. $\{k, \ell\} = \{-3.0, 0.5\}$.   (f) IV$_2$. $\{k, \ell\} = \{-3.0, -0.5\}$.

FIG. 2: The ground-state diagrams for the FM case ($j = +1$). (a) The $\{k, \ell\}$ plane, showing in different colors the five regions corresponding to the topologically different ground-state diagrams in the $\{h, d\}$ plane. The line $k = 1$ ($\phi_{AB} = 0$) corresponds to the lower left half-plane in Fig. 3 of Ref. [7]. (b − f) The ground-state diagrams in each region, with the specific values of $\{k, \ell\}$ used to generate each example. These points are marked by solid black circles in part (a).
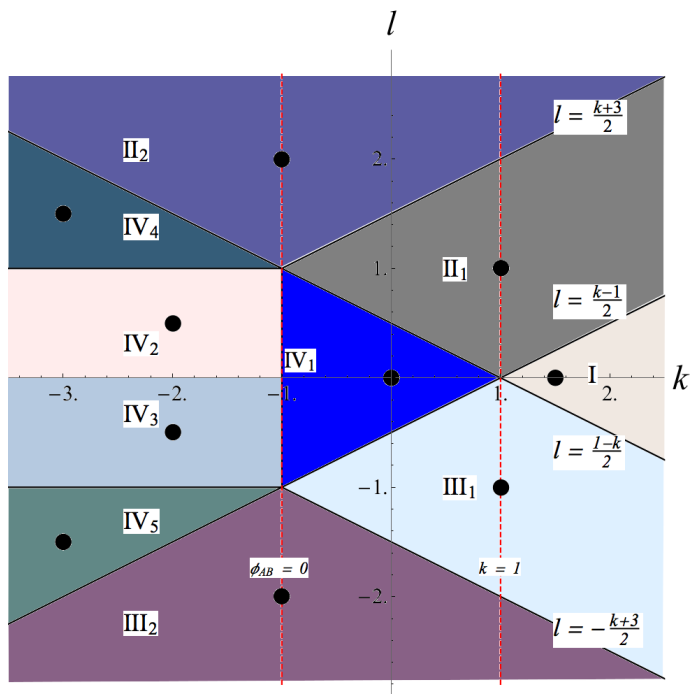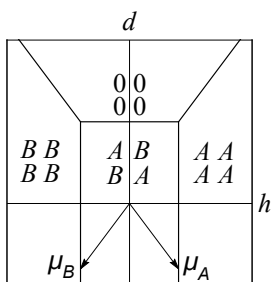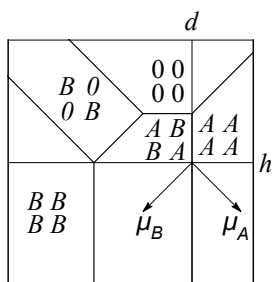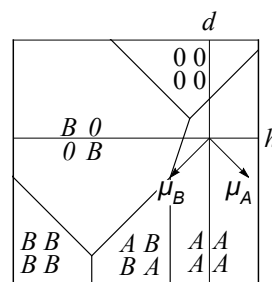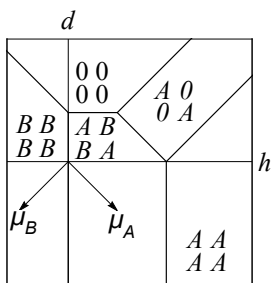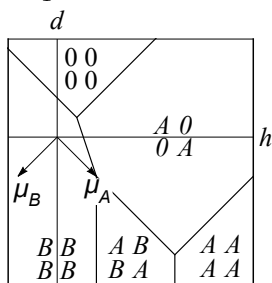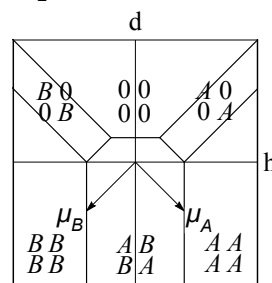
11

(a) The regions in the $\{k, \ell\}$ plane in the AFM case.

(b) I. $\{k, \ell\} = \{0.5, 0.0\}$.

(c) II$_1$. $\{k, \ell\} = \{1.0, 0.5\}$.

(d) II$_2$. $\{k, \ell\} = \{-1.0, 2.0\}$.

(e) III$_1$. $\{k, \ell\} = \{1.0, -0.5\}$.

(f) III$_2$. $\{k, \ell\} = \{-1.0, -2.0\}$.

(g) IV$_1$. $\{k, \ell\} = \{0.0, 0.0\}$.

FIG. 3: Continued on next page.

(h) IV_2. $\{k, \ell\} = \{-2.0, 0.5\}$. (i) IV_3. $\{k, \ell\} = \{-2.0, -0.5\}$.

(j) IV_4. $\{k, \ell\} = \{-3.0, 1.5\}$. (k) IV_5. $\{k, \ell\} = \{-3.0, -1.5\}$.
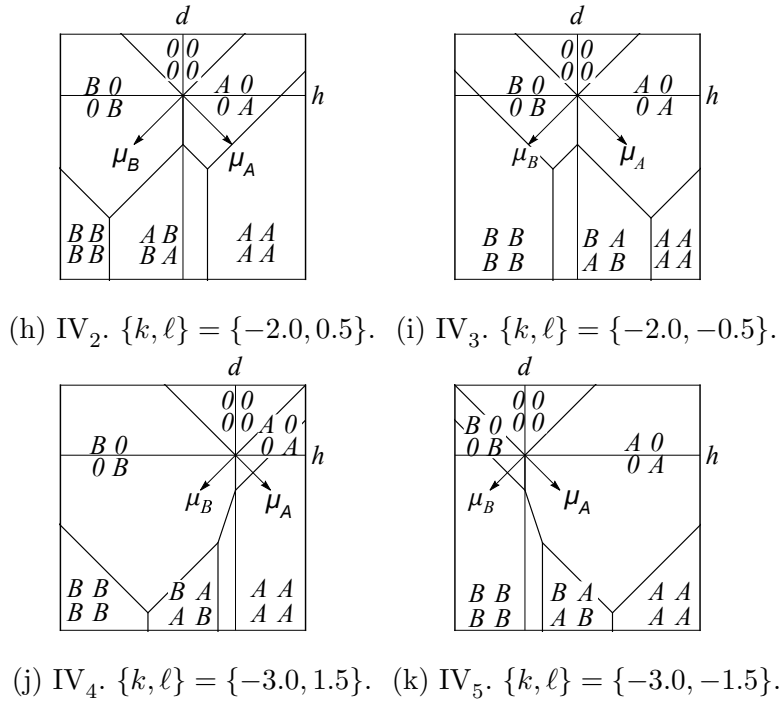
FIG. 3: The ground-state diagrams for the AFM case ($j = -1$). (a) The $\{k, \ell\}$ plane, showing in different colors the ten regions corresponding to the topologically different ground-state diagrams in the $\{h, d\}$ plane. The line $k = -1$ ($\phi_{AB} = 0$) corresponds to the upper right half-plane in Fig. 3 of Ref. [7]. (b – k) The ground-state diagrams in each region, with the specific values of $\{k, \ell\}$ used to generate each example. These points are marked by solid black circles in part (a).

The four main regions in the $\{k, \ell\}$ plane for both the FM or AFM cases correspond to the asymptotic behaviors for large $-\mu_A$ or $-\mu_B$. In both cases, this causes the Hamiltonian to reduce to an effective $S = 1/2$ Ising model. For large $-\mu_A$ the ground-state diagram is symmetric about $\mu_B = -2(J + K - 2L) = -2\phi_{BB}$. For large $-\mu_B$ the ground-state diagram is symmetric about the line $\mu_A = -2(J + K + 2L) = -2\phi_{AA}$. Each of these limits may be FM or AFM in the $D \to -\infty$ limit, depending on whether J is positive or negative. This leads to four different ways to combine the asymptotic behaviors for $-\mu_A$ and $-\mu_B$.

In Fig. 2 we show in part (a) the five regions in the $\{k, \ell\}$ plane for the FM case, with examples of the corresponding ground-state diagrams illustrated in parts (b-f). The line $k = 1$ ($\phi_{AB} = 0$), which cuts through regions I, II, and III, corresponds to the lower left

half-plane in Fig. 3 of Ref. [7]. In the FM case ($j = +1$) shown here, restriction to this line excludes the possibility of both ϕ_{AA} and ϕ_{BB} being negative, which corresponds to main region IV in this figure.

In Fig. 3 we show in part (a) the ten regions in the $\{k, \ell\}$ plane for the AFM case, with examples of the corresponding ground-state diagrams illustrated in parts (b-k). The ground-state diagram for the AFM BC model corresponds to the origin, which lies at the center of region IV_1. It was previously presented in Ref. [17] in the context of a study of the tricritical properties of this model at nonzero temperatures. The line $k = -1$ ($\phi_{AB} = 0$), which cuts through regions II_2 and III_2 and corresponds to the border between region IV_1 and regions IV_2 and IV_3, corresponds to the upper right half-plane in Fig. 3 of Ref. [7]. It does not include the topologically different ground-state diagrams in regions I, II_1, III_1, IV_4, and IV_5.

In both Figs. 2 and 3, the equations that mark the transition lines between pairs of ground states in the $\{h, d\}$ plane are omitted for readability. They are calculated by pairwise equating the energies per site that are given in Table I, and they are shown in Table III in both LG and Ising notation.

IV. SUMMARY AND CONCLUSIONS

The ground-state diagram for a statistical-mechanical model provides a solid foundation for studies of equilibrium and nonequilibrium phenomena at nonzero temperature. In this paper we therefore present a complete catalog of the fifteen topologically different ground-state diagrams for the most general three-state LG or equivalently $S = 1$ Ising model with only nearest-neighbor interactions on a square lattice. Each individual ground-state diagram shows the lines in the $\{h, d\}$ plane that separate the regions of stability of different ground states within a particular region of the reduced interaction parameters, $\{j = \pm 1, k, \ell\}$.

This model is often used to study phase transitions in two-component adsorption at solid-gas and solid-liquid interfaces, as well as in magnetic and dielectric spin systems, and it provides a rich laboratory for studying a number of critical and multicritical phenomena within the framework of one single model. The square lattice has important physical realizations as the (100) planes of face-centered and body-centered cubic crystals, and it is also often used as a simple basis for theoretical studies.

TABLE III: Equations for direct transition lines between pairs of ground states. The table has the form of a symmetric matrix. The ground state $(\sqrt{2}\times\sqrt{2})^1_0$ is realized only in the AFM case ($J<0$). Analogously, $(\sqrt{2}\times\sqrt{2})^{1/2}_{1/2}$ is only a possible ground state if $\phi_{AA}<0$, and $(\sqrt{2}\times\sqrt{2})^{1/2}_{-1/2}$ requires $\phi_{BB}<0$. These requirements are direct consequences of Eqs. (12–14).

Config.	State	$(1\times1)^1_1$	$(1\times1)^1_{-1}$	$(1\times1)^0_0$	$(\sqrt{2}\times\sqrt{2})^1_0$	$(\sqrt{2}\times\sqrt{2})^{1/2}_{1/2}$	$(\sqrt{2}\times\sqrt{2})^{1/2}_{-1/2}$
AA	$(1\times1)^1_1$		$H=-4L$	$D=H+2(J+K+2L)$	$H=-4L-4J$	$D=H+4(J+K+2L)$	$D=3H+4(J+K+2L)$
AA			$\mu_A-\mu_B=-2(\phi_{AA}-\phi_{BB})$	$\mu_A=-2\phi_{AA}$	$\mu_A-\mu_B=-4(\phi_{AA}-\phi_{AB})$	$\mu_A=-4\phi_{AA}$	$2\mu_A-\mu_B=-4\phi_{AA}$
BB	$(1\times1)^1_{-1}$	$H=-4L$		$D=-H+2(J+K-2L)$	$H=-4L+4J$	$D=-3H+4(J+K-2L)$	$D=-H+4(J+K-2L)$
BB		$\mu_A-\mu_B=-2(\phi_{AA}-\phi_{BB})$		$\mu_B=-2\phi_{BB}$	$\mu_A-\mu_B=4(\phi_{BB}-\phi_{AB})$	$\mu_A-2\mu_B=4\phi_{BB}$	$\mu_B=-4\phi_{BB}$
00	$(1\times1)^0_0$	$D=H+2(J+K+2L)$	$D=-H+2(J+K-2L)$		$D=2(-J+K)$	$D=H$	$D=-H$
00		$\mu_A=-2\phi_{AA}$	$\mu_B=-2\phi_{BB}$		$\mu_A+\mu_B=-4\phi_{AB}$	$\mu_A=0$	$\mu_B=0$
AB	$(\sqrt{2}\times\sqrt{2})^1_0$	$H=-4L-4J$	$H=-4L+4J$	$D=2(-J+K)$		$D=-H+4(-J+K)$	$D=H+4(-J+K)$
BA		$\mu_A-\mu_B=-4(\phi_{AA}-\phi_{AB})$	$\mu_A-\mu_B=4(\phi_{BB}-\phi_{AB})$	$\mu_A+\mu_B=-4\phi_{AB}$		$\mu_B=-4\phi_{AB}$	$\mu_A=-4\phi_{AB}$
A0	$(\sqrt{2}\times\sqrt{2})^{1/2}_{1/2}$	$D=H+4(J+K+2L)$	$D=-3H+4(J+K-2L)$	$D=H$	$D=-H+4(-J+K)$		$H=0$
0A		$\mu_A=-4\phi_{AA}$	$\mu_A-2\mu_B=4\phi_{BB}$	$\mu_A=0$	$\mu_B=-4\phi_{AB}$		$\mu_A=\mu_B$
B0	$(\sqrt{2}\times\sqrt{2})^{1/2}_{-1/2}$	$D=3H+4(J+K+2L)$	$D=-H+4(J+K-2L)$	$D=-H$	$D=H+4(-J+K)$	$H=0$	
0B		$2\mu_A-\mu_B=-4\phi_{AA}$	$\mu_B=-4\phi_{BB}$	$\mu_B=0$	$\mu_A=-4\phi_{AB}$	$\mu_A=\mu_B$	

The model is defined in a five-dimensional parameter space consisting of three interaction constants and two external chemical potentials or fields. Six topologically different ground-state diagrams for this model in a subspace with only two independent interaction constants were recently published [7], but we are not aware of previous publication of a complete catalog for the full, five-dimensional parameter space. We thus feel that our results fill a void, and we hope that they will be useful for future research in physical chemistry and chemical physics at interfaces.

CONFLICTS OF INTEREST

There are no conflicts to declare.

ACKNOWLEDGMENTS

[1] E. Ising, Beitrag zur Theorie des Ferromagnetismus, *Z. Physik*, 1925, **31**, 253-258.

[2] L. Onsager, Crystal statistics. I. A two-dimensional model with an order-disorder transition, *Phys. Rev.*, 1944, **65**, 117-149.

[3] E. Ibarra-García-Padilla, C. G. Malanche-Flores, and F. J. Povedo-Cuevas, The hobbyhorse of magnetic systems: the Ising model, *Eur. J. Phys.*, 2016, **37**, 065103.

[4] D. Stauffer, Social applications of two-dimensional Ising models, *Am. J. Phys.*, 2008, **76**, 470-473.

[5] H. W. Capel, On the possibility of first-order phase transitions in Ising systems of triplet ions with zero-field splitting, *Physica*, 1966, **32**, 966-988.

[6] M. Blume, V. J. Emery, and R. B. Griffiths, Ising model for the λ transition and phase separation in He^3-He^4 mixtures, *Phys. Rev. A*, 1971, **4**, 1071-1077.

[7] V. F. Fefelov, A. V. Myshlyavtsev, and M. D. Myshlyavtseva, Phase diversity in an adsorption model of an additive binary gas mixture for all sets of lateral interactions, *Phys. Chem. Chem. Phys.*, 2018, **20**, 10359-10368.

[8] P. A. Rikvold, J. B. Collins, G. D. Hansen, and J. D. Gunton, Three-state lattice gas on a triangular lattice as a model for multicomponent adsorption, *Surf. Sci.*, 1988, **203**, 500-524.

[9] J. B. Collins, P. Sacramento, P. A. Rikvold, and J. D. Gunton, Lateral interactions in catalyst poisoning, *Surf. Sci.*, 1989, **221**, 277-298.

[10] P. A. Rikvold, J. Zhang, Y.-E. Sung, and A. Wieckowski, Lattice-gas models of adsorption in the double layer, *Electrochim. Acta*, 1996, **41**, 2175-2184.

[11] K. H. O. Hasnaoui and J. Piekarewicz, Charged Ising model of neutron star matter, *Phys. Rev. C*, 2013, **88**, 025807.

[12] J. B. Collins, P. A. Rikvold, and E. T. Gawlinski, Finite-size scaling analysis of the $S = 1$ Ising model on the triangular lattice, *Phys. Rev. B*, 1988, **38**, 6741-6750.

[13] D. A. Huckaby and J. M. Kowalski, Phase transitions in a lattice gas model for coadsorption, *J. Chem. Phys.*, 1984, **80**, 2163-2167.

[14] N. De La Espriella, G.M. Buendía, and J.C. Madera, Mixed spin-1 and spin-2 Ising model: study of the ground states, *J. Phys. Commun.*, 2018, **2**, 025006.

[15] E. Domany, M. Schick, J. S. Walker, and R. B. Griffiths, Classification of continuous order-disorder transitions in adsorbed monolayers, *Phys. Rev. B*, 1978, **18**, 2209-2217.

[16] M. Schick, The classification of order-disorder transitions on surfaces, *Prog. Surf. Sci.*, 1981, **11**, 245-292.

[17] J. D. Kimel, P. A. Rikvold, and Y.-L. Wang, Phase diagram for the antiferromagnetic Blume-Capel model near tricriticality, *Phys. Rev. B*, 1992, **45**, 7237-7243.

This file contains the graphic and text Table of Contents entry
for manuscript CP-ART-12-2018-007721
Complete catalog of ground-state diagrams for the general three-state lattice-gas model with nearest-neighbor interactions on a square lattice
By Daniel Silva and Per Arne Rikvold
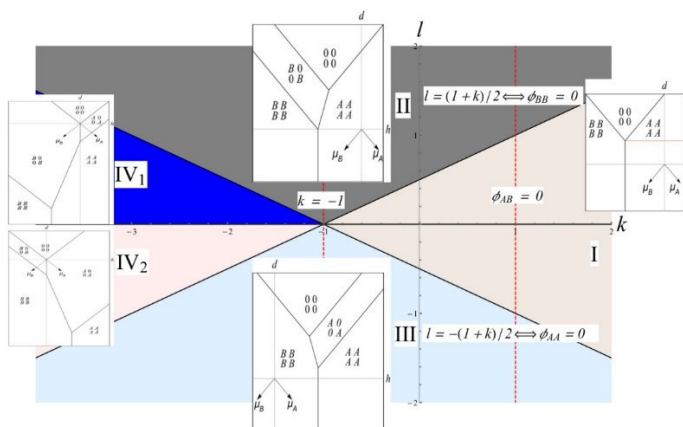
The fifteen topologically different zero-temperature phase diagrams in the model's full, five-dimensional parameter space provide a solid foundation for studies at finite temperatures.